ISSN 1674-1056
http://cpb.iphy.ac.cn
http://iopscience.iop.org/cpb
中国物理 B
Chinese Physics
中国物理 Chinese Physics B

Micromagnetism simulation on effects of soft phase size on $Nd_2Fe_{14}B/\alpha$ –Fe nanocomposite magnet with soft phase imbedded in hard phase

Yu-Qing Li(李玉卿), Ming Yue(岳明), Yi Peng(彭懿), Hong-Guo Zhang(张红国)

Citation: Chin. Phys. B . 2018, 27(8): 087502. **doi:** 10.1088/1674-1056/27/8/087502

Journal homepage: http://cpb.iphy.ac.cn; http://iopscience.iop.org/cpb

What follows is a list of articles you may be interested in

Anisotropic nanocomposite soft/hard multilayer magnets

Wei Liu(刘伟), Zhidong Zhang(张志东)

Chin. Phys. B . 2017, 26(11): 117502. **doi:** 10.1088/1674-1056/26/11/117502

Effects of spacer layers on magnetic properties and exchange couplings of Nd-Fe-B/Nd-Ce-Fe-B multilayer films

Ya-Chao Sun(孙亚超), Ming-Gang Zhu(朱明刚), Wei Liu(刘伟), Rui Han(韩瑞), Wen-Chen Zhang(张文臣), Yan-Feng Li(李岩峰), Wei Li(李卫)

Chin. Phys. B . 2017, 26(10): 107501. **doi:** 10.1088/1674-1056/26/10/107501

Abnormal variation of magnetic properties with Ce content in $(PrNdCe)_2Fe_{14}B$ sintered magnets prepared by dual alloy method

Xue-Feng Zhang(张雪峰), Jian-Ting Lan(兰剑亭), Zhu-Bai Li(李柱柏), Yan-Li Liu(刘艳丽), Le-Le Zhang(张乐乐), Yong-Feng Li(李永峰), Qian Zhao(赵倩)

Chin. Phys. B . 2016, 25(5): 057502. **doi:** 10.1088/1674-1056/25/5/057502

Evolution of structure and magnetic properties in $PrCo_5$ magnet for high energy ball milling in ethanol

Li Zhu-Bai, Lan Jian-Ting, Zhang Xue-Feng, Liu Yan-Li, Li Yong-Feng

Chin. Phys. B . 2015, 24(8): 087501. **doi:** 10.1088/1674-1056/24/8/087501

High frequency magnetic properties of ferromagnetic thin films and magnetization dynamics of coherent precession

Jiang Chang-Jun, Fan Xiao-Long, Xue De-Sheng

Chin. Phys. B . 2015, 24(5): 057504. **doi:** 10.1088/1674-1056/24/5/057504

Micromagnetism simulation on effects of soft phase size on $Nd_2Fe_{14}B/\alpha$–Fe nanocomposite magnet with soft phase imbedded in hard phase*

Yu-Qing Li(李玉卿), Ming Yue(岳明)†, Yi Peng(彭懿), and Hong-Guo Zhang(张红国)

College of Materials Science and Engineering, Beijing University of Technology, Beijing 100124, *China*

(Received 18 January 2018; revised manuscript received 25 April 2018; published online 25 July 2018)

In this study, micromagnetism simulation by using finite difference method is carried out on the $Nd_2Fe_{14}B/\alpha$-Fe nanocomposite magnet with soft phase imbedded in hard phase. The effects of soft magnetic phase size (S) on the magnetic properties and magnetic reversal modes are systematically analyzed. As S increases from 1 nm to 48 nm, the remanence (J_r) increases, while the coercivity (H_{ci}) decreases, leading to the result that the magnetic energy product [$(BH)_{max}$] first increases slowly, and then decreases rapidly, peaking at $S = 24$ nm with the $(BH)_{max}$ of 72.9 MGOe (1 MGOe = 7.95775 kJ·m^{-3}). Besides, with the increase of S, the coercivity mechanism of the nanocomposite magnet changes from nucleation to pinning. Furthermore, by observing the magnetic moment evolution in demagnetization process, the magnetic reversal of the soft phase in the nanocomposite magnet can be divided into three modes with the increase of S: coherent rotation ($S < 3$ nm), quasi-coherent rotation (3 nm $\leqslant S <$ 36 nm), and the vortex-like rotation ($S \geqslant 36$ nm).

Keywords: micromagnetism simulation, magnetization dynamics, $Nd_2Fe_{14}B/\alpha$–Fe nanocomposite magnets

PACS: 75.78.Cd, 75.78.–n, 75.90.+w **DOI:** 10.1088/1674-1056/27/8/087502

1. Introduction

Nanocomposite permanent magnets are an important research focus in the field of permanent magnetic materials for the potential of obtaining extraordinary magnetic properties.[1–4] After decades of development, a series of successes[1–22] has been achieved in both experiment and micromagnetic simulations for nanocomposite magnets. Firstly, the researchers have predicted the high theoretical energy product of the nanocomposite magnet by micromagnetic simulation. Giant theoretical energy products of 137 MGOe, 90 MGOe, 65 MGOe, and 25 MGOe were acquired from the $Sm_2Fe_{17}N_3/Fe_{65}Co_{35}$,[1] $Nd_2Fe_{14}B/Fe_{65}Co_{35}$,[2] $SmCo_5/Fe$,[3] and MnBi/FeCo[4] nanocomposite magnets, respectively. Besides, excellent magnetic properties exceeding the corresponding single hard phase magnets have been achieved from experimental preparation nanocomposite multilayers. Cui *et al.*[5] reported that the high energy product of 486 kJ/m^3 (61 MGOe) based on the Nd–Fe–B/FeCo nanocomposite multilayers is higher than the maximum experimental energy product of single-phase Nd–Fe–B magnet. Moreover, Nev *et al.*[6] obtained the energy product exceeding 50 MGOe based on SmCo5/α Fe multilayers, which is much higher than the theorical energy product (30 MGOe) of single $SmCo_5$ magnet. However, magnetic film is difficult to practically use massively due to the limitation of their sizes. Instead, the bulk magnets are always the research hotspot in the field of permanent magnet for their application prospects. A lot of experimental and theoretical research progress has been reported for the bulk nanocomposite magnets.[7–9] Recently, Zhang *et al.*[10] reported inspiring results that the bulk SmCo/FeCo nanocomposite magnets have acquired the $(BH)_{max}$ of 28 MGOe which is 46% enhancement in energy product compared with the corresponding pure rare-earth magnets. One of the pivotal problems to obtain high magnetic properties for bulk nanocomposite magnets is that it is hard to obtain fine soft magnetic phase by using the current technology. Fortunately, the micromagnetic simulation analysis method can be used to explore the magnetic properties, coercivity mechanism and magnetic reversal process for nanocomposite magnet. Leineweber and Kronmüller[2,13] calculated the thickness-dependent remanence, nucleation field and energy product of the soft phase for the $Nd_2Fe_{14}B/\alpha$–Fe multilayers. Zhang *et al.*[14] simulated the effects of grain size and texture on the magnetic properties and the magnetic reversal behavior of three-dimensional (3D) nanocomposite magnet by micromagnetic finite element. It was also found in our previous work[15] that all the demagnetization curves with thickness in a range of 2 nm–30 nm of the perpendicular orientation trilayers exhibit "single phase" behavior, while noticeable kinks are present in the demagnetization curves of the parallel orientation $Nd_2Fe_{14}B/Fe_{65}Co_{35}/Nd_2Fe_{14}B$ trilay-

*Project supported by the Key Program of the National Natural Science Foundation of China (Grant No. 51331003), the International S & T Cooperation Program of China (Grant No. 2015DFG52020), the General Program of Science and Technology Development Project of Beijing Municipal Education Commission, China (Grant No. KM201710005006), and the State Key Laboratory of Advanced Metals and Materials, China (Grant No. 2015-ZD02).

†Corresponding author. E-mail: yueming@bjut.edu.cn

© 2018 Chinese Physical Society and IOP Publishing Ltd

ers with the soft phase thickness equal to or larger than 12 nm. The same phenomenon was also found in the micromagnetic simulation results of 3D $Nd_2Fe_{14}B/\alpha$–Fe multilayers.[16] Cui *et al.*[17] reported that coupling effects between the soft and hard phase of the perpendicular orientation multilayers due to the exchange interaction and magnetostatic interaction, while the coupling effects in the parallel orientation multilayers only result from the exchange interaction. For 3D bulk magnet, there is a great difference in complex microstructure where the two coupling effects of perpendicular orientation and parallel orientation coexist. So, the critical size of the soft phase is also different from that obtained from the classical one-dimensional (1D) model. In this study, the influence of soft phase size (S) on magnetic properties and magnetic reversal of the simple 3D $Nd_2Fe_{14}B/\alpha$–Fe nanocomposite magnet with soft phase imbedded in hard phase can be analyzed by micromagnetic simulation. On this account, the theoretical basis can be provided for the selection/control of the size of soft phase in the experimental preparation of the bulk nanocomposite magnets.

2. Simulated model and method

The software OOMMF[18] is used in this calculation. OOMMF is one of the micromagnetic calculation software which is based on the Landau–Lifshitz–Gilbert (LLG) dynamic equation[16]

$$\frac{\mathrm{d}\boldsymbol{M}}{\mathrm{d}t} = -|\overline{\gamma}|\,\boldsymbol{M}\times\boldsymbol{H}_{\mathrm{eff}} - \frac{|\overline{\gamma}|\,\alpha}{M_{\mathrm{S}}}\times(\boldsymbol{M}\times\boldsymbol{H}_{\mathrm{eff}}), \qquad (1)$$

where $\boldsymbol{M}$ is the magnetization, $\boldsymbol{H}_{\mathrm{eff}}$ is the effective field (in units A/m), $|\overline{\gamma}|$ is the Landau–Lifshitz gyromagnetic ratio, and α is the damping coefficient (dimensionless). α is set to be 0.5 in our calculation to make a good balance between the calculation precision and speed.[16] The effective field (H_{eff}) is defined as

$$H_{\mathrm{eff}} = -\mu_0^{-1}\frac{\partial E_{\mathrm{tot}}}{\partial M}. \qquad (2)$$

The totally energy density (E_{tot}) can be considered as

$$E_{\mathrm{tot}} = E_{\mathrm{H}} + E_{\mathrm{D}} + E_{\mathrm{K}} + E_{\mathrm{ex}}, \qquad (3)$$

where E_{H}, E_{D}, E_{K}, and E_{ex} are zeeman energy in external field, demagnetization energy, anisotropy energy, and exchange energy,[19–21] respectively.

In this paper, we consider $Nd_2Fe_{14}B/\alpha$–Fe nanocomposite magnets with the following intrinsic magnetic parameters:[19,22] for saturated magnetization, $J_{\mathrm{s}}(Nd_2Fe_{14}B) = 1.61$ T, $J_{\mathrm{s}}(\mathrm{Fe}) = 2.15$ T, for anisotropic constant $K_1(Nd_2Fe_{14}B) = 4.331$ MJ/m^3, $K_1(\mathrm{Fe}) = 0.046$ MJ/m^3, and for integral exchange constant $A(Nd_2Fe_{14}B) = 0.77\times10^{-11}$ J/m, $A(\mathrm{Fe}) = 2.5\times10^{-11}$ J/m.

Figure 1 shows the schematic diagram of simulated model for the soft phase (core) imbedded in hard phase (shell) $Nd_2Fe_{14}B/\alpha$–Fe nanocomposite magnets. Our calculation model is based on an o-xyz coordinate system. Both the magnetocrystalline anisotropic easy axis (e) and the applied field (H) are assumed to be in the z-axis direction as shown in Fig. 1(a). The simulation model is cubic. The white represents hard phase and the thickness (H) is set to be 8 nm, while the red represents soft phase and the thickness (S) changes from 1 nm to 48 nm as shown in Fig.1(b). For the $Nd_2Fe_{14}B/\alpha$–Fe nanocomposite magnets, the size of the theoretical $Nd_2Fe_{14}B$ domain wall is about 4 nm. So, in this paper, to ensure accurate calculation, the simulation mesh is 1 nm × 1 nm × 1 nm, except the mesh size of 0.5 nm × 0.5 nm × 0.5 nm that is used for $S = 1$-nm samples.

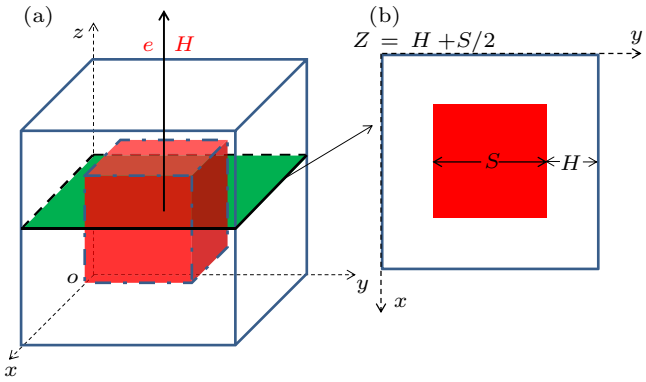


Fig. 1. (color online) Schematic diagram of $Nd_2Fe_{14}B/\alpha$–Fe nanocomposite magnets with soft phase imbedded in hard phase, showing (a) 3D schematic diagram based on the o–xyz coordinate, with e and H representing easy axis and applied field respectively, and (b) green cross section in panel (a), with H being thickness of hard phase and S denoting thickness of soft phase.

3. Results and discussion

Figure 2 shows the hysteresis loops of the $Nd_2Fe_{14}B/\alpha$–Fe nanocomposite magnets with soft phase imbedded in hard phase. The hysteresis loops of the $Nd_2Fe_{14}B/\alpha$–Fe nanocomposite magnets show excellent squareness with S from 1 nm to 4 nm. But it is noticeable that the deterioration of quareness appears and turns more and more obvious with the increase of S as shown in Fig. 2. In addition, when $S = 48$ nm, there is an obvious kink near the coercive field, indicating the non-uniform magnetic reversal.

Figure 3 shows the S-dependent saturation magnetization (J_{s}), remanence (J_{r}), and maximum energy product [$(\mathrm{BH})_{\mathrm{max}}$] of the $Nd_2Fe_{14}B/\alpha$–Fe nanocomposite magnets. With the increase of S, the J_{s} ($J_{\mathrm{s}} = V_{\mathrm{s}}J_{\mathrm{s}} + V_{\mathrm{h}}J_{\mathrm{h}}$) increases from 16.1 kGs ($S = 1$ nm) to 18.4 kGs ($S = 48$ nm) (1 Gs = 10^{-4} T), while the remanence increases from 16.1 kGs ($S = 1$ nm) to 18.3 kGs ($S = 48$ nm), respectively. The high remanence ratio ($J_{\mathrm{r}}/J_{\mathrm{s}}$) in the range of S of 1 nm–48 nm indicates the significant remanence enhancement effect, which results from good exchange coupling interaction and magnetostatic interaction between

soft and hard phase.[17] The $(BH)_{max}$ of the $Nd_2Fe_{14}B/\alpha$–Fe nanocomposite magnets rises slowly and then decreases rapidly as the S increases, resulting in peaking at $S = 24$ nm with maximum $(BH)_{max}$ of 72.9 MGOe as shown in Fig. 3. Generally, the size of soft phase should not exceed twice the domain wall width of the neighboring hard phase to guarantee the good exchange coupling effect based on classic1D model with parallel orientation.[23] This means that the size of α-Fe should be smaller than 8.4 nm for $Nd_2Fe_{14}B/\alpha$–Fe nanocomposite magnets. However, the studies[17,24] of micromagnetic simulation and experimental work shows that the nanocomposite magnetic films with parallel orientation (the axis is parallel to the film surface) are decoupling for too large soft phase size, while the perpendicular orientation films can be coupled even the size of the soft magnetic phase is large. The 3D model can be regarded as the combination of parallel orientation and perpendicular orientation nanocmposite films. The simulation results in the present paper show that the maximum magnetic energy product can be obtained in the bulk nanocomposite magnets when the size of single soft phase particle is 24 nm.

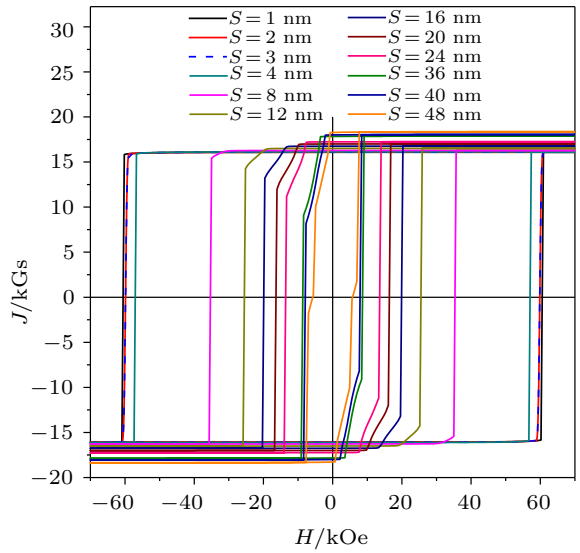


Fig. 2. (color online) Simulated hysteresis loops of $Nd_2Fe_{14}B/\alpha$–Fe nanocomposite magnets with soft imbedded in hard phase for various S values.

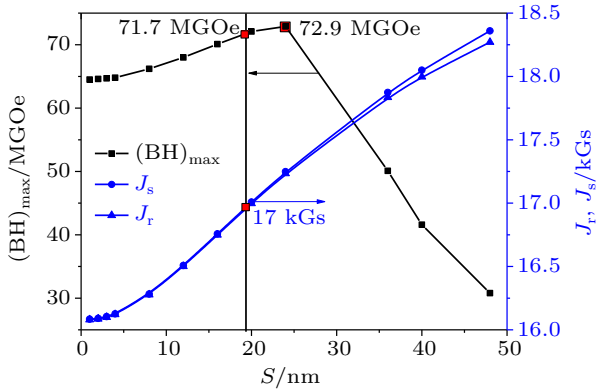


Fig. 3. (color online) S-dependent J_s, J_r and $(BH)_{max}$ of $Nd_2Fe_{14}B/\alpha$–Fe nanocomposite magnets with soft phase imbedded in hard phase.

Figure 4 shows the S-dependent coercivity (H_{ci}) and nucleation field (H_n) of the $Nd_2Fe_{14}B/\alpha$–Fe nanocomposite magnets. The H_{ci} decreases monotonically from 60.6 kOe (1 Oe = 79.5775 A·m^{-1}) ($S = 1$ nm) to 5.6 kOe ($S = 48$ nm). The nucleation field (H_n) is defined as the absolute value of applied field (H) where the magnetic moment deflection begins to occur. With S in a range from 1 nm to 4 nm, the H_{ci} is almost equal to the H_n, that is to say, the reverse nucleation and reversal occur simultaneously, suggesting that the dominant coercivity mechanism of the $Nd_2Fe_{14}B/\alpha$–Fe nanocomposite magnets with $S \leqslant 4$ nm is nucleation. Then, as $S > 4$ nm, the H_{ci} is always larger than H_n, and the discrepancy between H_{ci} and H_n, increases with the increase of S. In other words, the reversal of magnetic moments lags behind the nucleation, indicating that the dominant coercivity mechanism of the nanocomposite magnet changes into pinning.

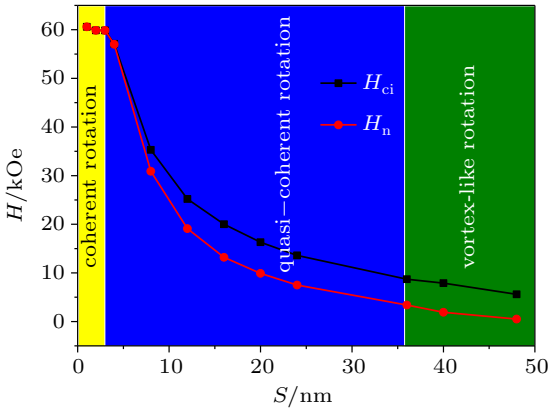


Fig. 4. (color online) S-dependent H_n, H_{ci} and magnetization reversal modes of $Nd_2Fe_{14}B/\alpha$–Fe nanocomposite magnets with soft phase imbedded in hard phase.

The magnetic moment evolution in magnetic reversal is also influenced by S, besides the effects of S on magnetic properties of nanocomposite magnets. Figure 3 also shows the relationship between the magnetic reversal mode and the size of soft phase particle of the $Nd_2Fe_{14}B/\alpha$–Fe nanocomposite magnets. By systematically observing the magnetic moment evolutions, the magnetic reversal of the nanocomposite magnets can be divided into three modes with the increase of S: coherent rotation ($S < 3$ nm), quasi-coherent rotation (3 nm $\leqslant S < 36$ nm), and vortex-like rotation ($S \geqslant 36$ nm) as shown in Fig. 4.

Figure 5 shows the spatial distributions of deflection angles (θ) for the nanocomposite magnets with $S = 2$ nm (coherent rotation), $S = 24$ nm (quasi-coherent rotation) and $S = 40$ nm (vortex-like rotation) when the nucleation and reversal occur. The θ means the deflection angle between magnetic moment and the easy axis. For magnet with $S = 2$ nm which shows the magnetic reversal mode of coherent rotation, the nucleation and irreversible reversal of the magnet occur simultaneously at $H = -59.5$ kOe. At the moment just before the nucleation occurs, the maximum θ is less than 7.5°.

Figure 6 shows the magnetic moment evolution of the magnet with $S = 2$ nm (coherent rotation) before and after the nucleation/reversal (in this paper, the observation plane is perpendicular to the applied field and/or easy axis, unless otherwise stated). For the magnets with coherent rotation reversal mode, the magnetic moments have only two states, $\theta = 0°$ and $\theta = 180°$. Once the nucleation occurs, the magnetic moments of hard phase and soft phase overturn simultaneously.

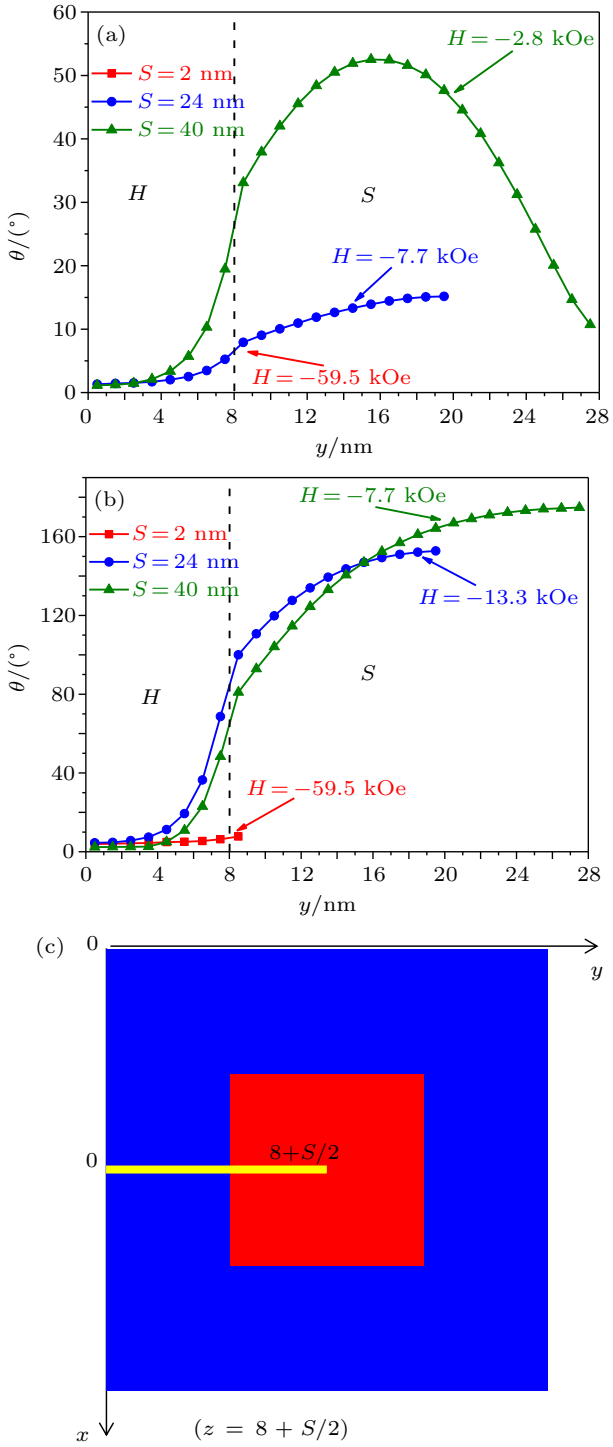


Fig. 5. (color online) Spatial distributions of magnetic moment deflection angles when (a) nucleation and (b) reversal occur, and (c) schematic diagram of corresponding magnetic moment position, with yellow line representing y axis in panels (a) and (b).

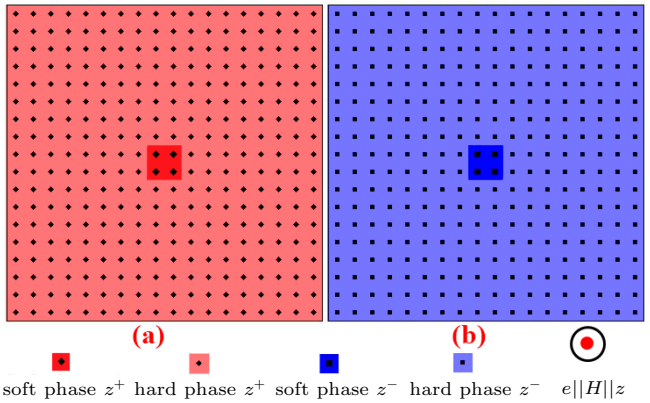


Fig. 6. (color online) Magnetic moment distributions of $Nd_2Fe_{14}B/\alpha$–Fe nanocomposite magnet with $S = 2$ nm, when (a) $H = -59.5$ kOe and (b) $H = -60.2$ kOe before and after reversal. Observation surface is xy plane and $z = 9$ nm.

The magnet with $S = 24$ nm shows the magnetic reversal mode of quasi-coherent rotation, and the nucleation and reversal occur at $H = -7.7$ kOe and $H = -13.3$ kOe, respectively. At the nucleation state, the maximum θ in the hard phase is about 5°, while the θ in the center of the soft phase is 15.1°. At the reversal state, the θ from the surface of the hard phase to the soft/hard phase interface increases from 0° to 68.2°, while the θ increases to 152.3° in the center of soft phase. Low nucleation field and large magnetic moment rotation at the reversal state lead to poor squareness of demagnetization curve, which is not conducive to obtaining high magnetic energy product. Figure 7 shows the magnetic moment evolution in magnetic reversal of the nanocomposite magnet with $S = 24$ nm (quasi-coherent rotation) at the nucleation and reversal states. For the nanocomposite magnets with quasi-coherent rotation reversal mode, the magnetic moment rotation occurs in the center of the soft phase, firstly. And then the magnetic moment rotation propagates gradually to the hard/soft interface with the decrease of H. Finally, reversal of the whole magnet occurs as shown in Fig. 7.

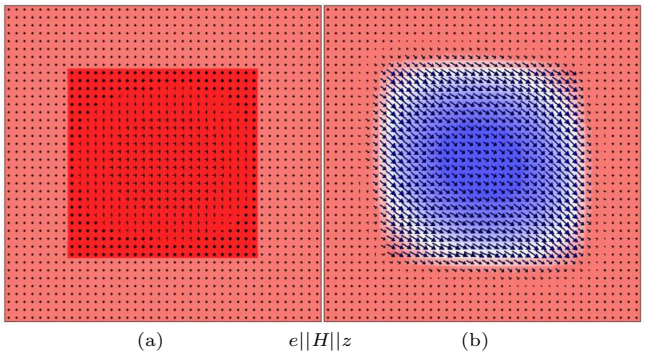


Fig. 7. (color online) Magnetic moment distributions of $Nd_2Fe_{14}B/\alpha$–Fe nanocomposite magnet with $S = 24$ nm, when (a) $H = -7.7$ kOe where nucleation occurs, and (b) $H = -13.3$ kOe before reversal of whole magnet. Observation surface is xy plane and $z = 20$ nm.

The nanocomposite magnet with $S = 40$ nm shows the magnetic reversal mode of vortex-like rotation, and the nucleation occurs at $H = -2.8$ kOe, while the reversal occurs at

$H = -7.7$ kOe. In the nucleation state, the θ from of the surface of hard phase to the soft/hard phase interface increases from 0° to 19.3°. Moreover, the θ increases first, then decreases from the soft/hard interface to the center of soft phase, peaking at $y = 16$ nm with a maximum θ of 52.5°. At the reversal state, the θ from the surface of the hard phase to the soft/hard phase interface increases from 0° to 48.0°, and the θ in the center of soft phase is about 174.4°. The large θ in both the hard and soft phase leads to low magnetic energy product even though the magnet bears a large $J_r = 18$ kGs. Figure 8 shows the magnetic moment evolution in magnetic reversal of the nanocomposite magnet with $S = 40$ nm (vortex-like rotation) at the nucleation and reversal state. As shown in Fig. 8, at the nucleation state, the magnetic moments are distributed like a circle featuring the vortex. Moreover, the θ increases first and then decreases with the increase of the radius of circular magnetic moments. This is the difference between vortex-like rotation in 3D $Nd_2Fe_{14}B/\alpha$–Fe nanocomposite magnets and vortex rotation[16] for the perpendicular orientation nanocomposite multilayer. For the 3D $Nd_2Fe_{14}B/\alpha$–Fe nanocomposite magnets, the soft phase is surrounded by hard phase in the direction both parallel and perpendicular to the easy axis. The magnetic moment of soft phase near the soft/hard interface is restricted by the exchange interaction in the direction parallel to the easy axis. After the nucleation, as the H decreases, the center of the vortex-like state begins to deviate from the center of the soft phase as shown in Fig. 8(b), indicating that the nucleation of vortex-like is unstable. As the H increases continuingly, the vortex-like state disappears and the reverse domains are formed as shown in Figs. 8(c) and 8(d).

As S increases to 48 nm, the magnetic reversal mode is also vortex-like rotation as shown in Fig. 9(a). The vortex-like nucleation becomes more stable than the magnet with $S = 40$ nm, because the center of the vortex-like nucleation does not move with the increase of H, only the θ increases continuously as shown in Fig. 9(b). However, it is worth noting that there is much difference in the reversal of the hard phase portion between the magnet with S =48 nm and the magnet with $S = 40$ nm. The reversals of hard phase parallel and perpendicular to the easy axis do not occur at the same time. Only the magnetic moments of hard phase perpendicular to the easy axis reverse when the reversal of soft phase happens as shown in Fig. 9(c). Meantime, the magnetic moments of hard phase parallel to the easy axis remain unchanged, indicating the pinning strengths in soft/hard interfaces parallel and perpendicular to the easy axis are different. Therefore, the magnetic reversals of nanocomposite magnets with $S = 48$ nm can be summarized as follow. Firstly, vortex-like nucleation appears in soft phase. Secondly, the deflection angles of the magnetic moments increase continuously. Thirdly, the magnetic moments of soft phase reverse together with the magnetic moments of the hard phase in the direction perpendicular

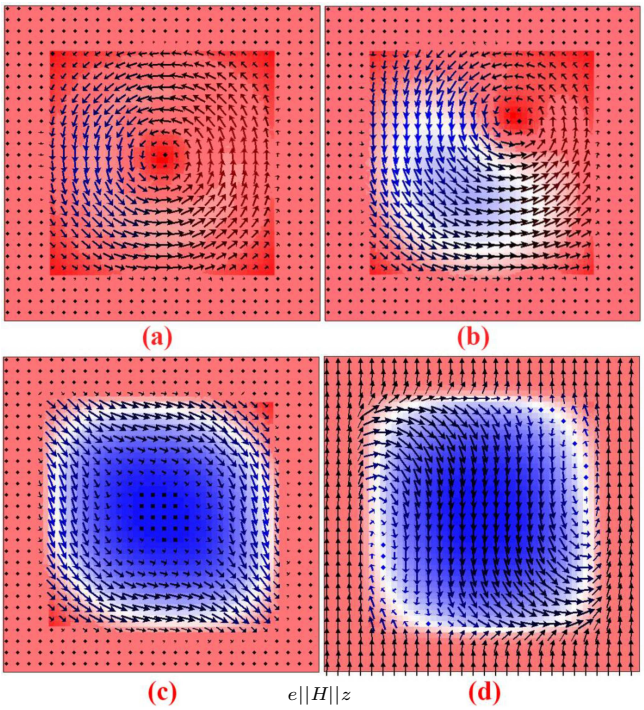


Fig. 8. (color online) Magnetic moment distributions of $Nd_2Fe_{14}B/\alpha$–Fe nanocomposite magnet with $S = 40$ nm, when (a) $H = -2.8$ kOe where nucleation occurs, (b) $H = -4.2$ kOe (b), $H = -7.7$ kOe before reversal of the whole magnet observation plane (c) perpendicular and (d) parallel to the easy axis. Observation surfaces of panels (a), (b) and (c) are xy plane and $z = 28$ nm while observation surfaces of panel (d) is xz plane and $y = 28$ nm.

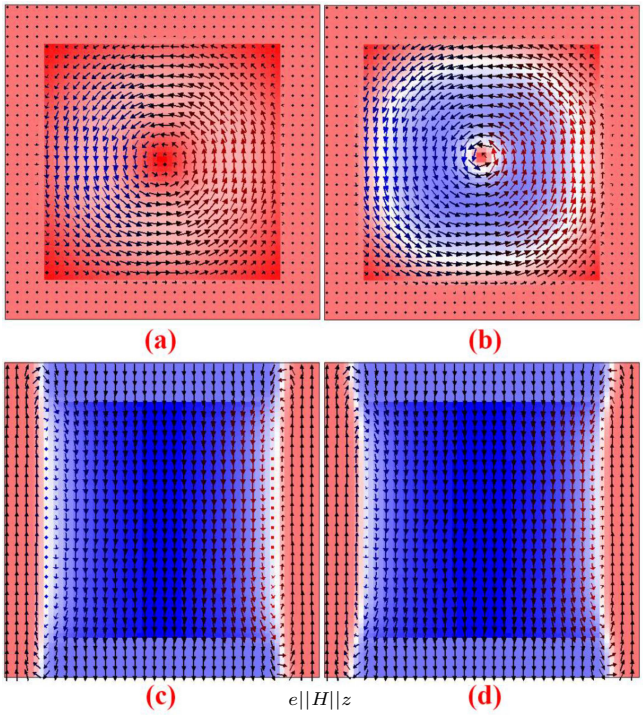


Fig. 9. (color online) Magnetic moment distributions of $Nd_2Fe_{14}B/\alpha$–Fe nanocomposite magnet with $S = 48$ nm, when (a) $H = -1.4$ kOe where the nucleation occurs, (b) $H = -4.9$ kOe, (c) $H = -5.6$ kOe after the reversal of hard phase perpendicular to the easy axis and (d) $H = -7$ kOe before the reversal of hard phase parallel to the easy axis, the observation surfaces of panels (a) and (b) are xy plane and $z = 32$ nm while the observation surfaces of panels (c) and (d) are xz plane and $y = 32$ nm.

to the easy axis. Finally, the magnetic moments of hard phase in the direction parallel to the easy axis reverse.

In order to meet the requirements for practical applications, the magnetic properties of the permanent magnet must be guaranteed that $H_{ci} \geqslant J_r$. For the $Nd_2Fe_{14}B/\alpha$–Fe nanocomposite magnets simulated in this paper, the critical S to meet requirements for practical application is 19.3 nm, falling in the region of quasi-coherent rotation. The corresponding $Nd_2Fe_{14}B/\alpha$–Fe nanocomposite magnet shows the magnetic properties of $J_r = 17$ kGs, $H_{ci} = 17$ kOe, and $(BH)_{max} = 71.7$ MGOe. When $S = 24$ nm, the $Nd_2Fe_{14}B/\alpha$–Fe nanocomposite magnet with soft phase imbedded in hard phase reaches a maximum $(BH)_{max}$ of 72.9 MGOe, which is just between the maximum calculated $(BH)_{max}$ values of perpendicular (67.9 MGOe for 1D, 68.5 MGOe for 3D) and parallel (79.1 MGOe for 1D, 75.1 MGOe for 3D) orientation 1D and 3D $Nd_2Fe_{14}B/\alpha$–Fe multilayers.[16,25]

In this paper, the hysteresis loop of $Nd_2Fe_{14}B/\alpha$–Fe nanocomposite magnet still maintains the characteristics of single phase permanent magnet, even if the size of soft phase (α-Fe) is larger than twice the width of domain wall for hard magnetic phase ($Nd_2Fe_{14}B$). In addition, when $S = 48$ nm, there are obvious kinks in the hysteresis loop due to the stepwise reversal of the hard phase.

For the 3D $Nd_2Fe_{14}B/\alpha$–Fe nanocomposite magnets with the soft phase imbedded in the hard phase, the magnetic reversal can be summarized in the following three processes: reverse domain nucleation in the center of soft phase, propagation of reverse domain walls, and pinning at the soft/hard interface, irreversible reversal of the whole sample, which is the same as the results in Refs. [16], [19], and [25] for the nanocomposite multilayers. With the increase of S, the mode of the soft magnetic nucleation is changed. In this paper, the reversal mode of the magnet is defined as the kind of nucleation mode. In addition, with the increase of S, the deflection of the soft magnetic phase becomes more and more serious, leading to the deterioration of the squareness of the hysteresis loop.

4. Conclusions

(i) The magnetic energy product $[(BH)_{max}]$ of the $Nd_2Fe_{14}B/\alpha$–Fe nanocomposite magnets with soft phase imbedded in hard phase peaks at $S = 24$ nm with a $(BH)_{max}$ of 72.9 MGOe.

(ii) As S increases, the dominant coercivity mechanism of the $Nd_2Fe_{14}B/\alpha$–Fe nanocomposite magnets with soft phase imbedded in hard phase changes from nucleation into pinning.

(iii) The hysteresis loops of $Nd_2Fe_{14}B/\alpha$–Fe nanocomposite magnets with S from 1 to 40 nm show the characteristics of single phase permanent magnet. For the $Nd_2Fe_{14}B/\alpha$–Fe nanocomposite magnet with $S = 48$ nm, the reversal of hard phase is divided into two portions due to the different pinning strengths of the soft/hard interface parallel and perpendicular to the easy axis.

(iv) The magnetic reversal mode of $Nd_2Fe_{14}B/\alpha$–Fe nanocomposite magnet with soft phase imbedded in hard phase can be divided into three modes with the increase of S: coherent rotation ($S < 3$ nm), quasi-coherent rotation (3 nm $\leqslant S < 36$ nm), and the vortex-like rotation ($S \geqslant 36$ nm).

References

[1] Skomski R and Coey J M D 1993 *Phys. Rev. B* **48** 15812
[2] Leineweber T and Kronmüller H 1997 *J. Magn. Magn. Mater.* **176** 145
[3] Sabiryanov R F and Jaswal S S 1998 *Phys. Rev. B* **58** 12071
[4] Li Y Q, Yue M, Wang T, Wu Q, Zhang D T and Gao Y 2015 *J. Magn. Magn. Mater.* **393** 484
[5] Cui W B, Takahashi Y K and Hono K 2012 *Adv. Mater.* **24** 6530
[6] Neu V, Sawatzki S, Kopte M, Mickel Ch and Schultz L 2012 *IEEE Trans. Magn.* **48** 3599
[7] Li H, Lou L, Hou F, Guo D, Li W, Li X, Gunderov D V, Sato K and Zhang X Y 2013 *Appl. Phys. Lett.* **103** 142406
[8] Liu Y, Xu L, Wang Q, Li W and Zhang X 2009 *Appl. Phys. Lett.* **94** 172502
[9] Rong C, Zhang Y, Poudyal N, Xiong X, Kramer M J and Liu J P 2010 *Appl. Phys. Lett.* **96** 102513
[10] Li X, Lou L, Song W, Huang G, Hou F, Zhang Q, Zhang H T, Xiao J, Wen B and Zhang X 2017 *Adv. Mater.* **29** 1606430
[11] Li X, Lou L, Song W, Zhang Q, Huang G, Hua Y, Zhang H T, Xiao J, Wen B and Zhang X 2017 *Nano Lett.* **17** 2985
[12] Li H, Li X, Guo D, Lou L, Li W and Zhang X 2016 *Nano Lett.* **16** 5631
[13] Leineweber T and Kronmüller H 1997 *Phys. Status Solidi B* **201** 291
[14] Zhang H W, Rong C B, Zhang S Y and Shen B G 2004 *Acta Phys. Sin.* **53** 4347 (in Chinese)
[15] Li Y Q, Yue M, Wu Q, Wang T, Cheng C X and Chen H X 2015 *J. Magn. Magn. Mater.* **394** 117
[16] Yuan X H, Zhao G P, Yue M, Ye L N, Xia J, Zhang X C and Chang J 2013 *J. Magn. Magn. Mater.* **343** 245
[17] Cui W B, Ma L, Sepehri-Amin H, Takahashi Y K and Hono K 2016 *Acta Mater.* **107** 49
[18] Donahue M J and Porter D G 1999 OOMMF *User's Guide*, Version 1.0 (Gaithersburg: National Institute of Standards and Technology)
[19] Zhao G P and Wang X L 2006 *Phys. Rev. B* **74** 012409
[20] Kronrniiller H and Goll D 2002 *Scr. Mater.* **47** 551
[21] Zhang H W, Rong C B, Zhang J, Zhang S Y and Shen B G 2002 *Phys. Rev. B* **66** 184436
[22] Zhao G P, Zhou G, Zhang H W, Feng Y P, Xian C W and Zhang Q X 2008 *Comp. Mater. Sci.* **44** 117
[23] Kneller E F and Hawing R 1991 *IEEE Trans. Magn.* **27** 3588
[24] Liu W and Zhang Z 2017 *Chin. Phys. B* **26** 117502
[25] Zhang W, Zhao G P, Yuan X H et al. 2012 *J. Magn. Magn. Mater.* **324** 4231